1,3-Dithiolane and 1,3-Ferrocenyl-dithiolane as Assembling Ligands for the Construction of Cu(I) Clusters and Coordination Polymers

Abhinav Raghuvanshi, Nakaw J. Dargallay, Michael Knorr, Lydie Viau, Lena Knauer, Carsten Strohmann

1,3-Dithiolane and 1,3-Ferrocenyl-dithiolane as Assembling Ligands for the Construction of Cu(I) Clusters and Coordination Polymers

Abhinav Raghuvanshi [a] • Nakaw J. Dargallay [a] • Michael Knorr *[a,] • Lydie Viau*[a] • Lena Knauer[b] • Carsten Strohmann*[b]

a) Institut UTINAM UMR CNRS 6213, Université Bourgogne Franche-Comté, F-25030 Besançon, France. Corresponding authors: E-mail: michael.knorr@univ-fcomte.fr ; lydie.viau@univ-fcomte.fr

b) Anorganische Chemie, Technische Universität Dortmund, Otto-Hahn-Strasse 6, D-44227 Dortmund, Germany. E-mail: carsten.strohmann@tu-dortmund.de

This paper is dedicated to Prof. Pierre D. Harvey in honor to his scientific achievements

ABSTRACT The parent compound 1,3-dithiolane **L1** reacts with CuI providing the 2D coordination polymer (CP) $[\{Cu(\mu_2\text{-}I)_2Cu\}(\mu_2\text{-}\mathbf{L1})_2]_n$ (**CP1**). The Cu···Cu distance within the $Cu(\mu_2\text{-}I)_2Cu$ rhomboid is temperature-dependent and shrinks from 2.9081(7) (294 K) to 2.8743(5) (100 K). The 1D polymeric compound $[\{Cu(\mu_2\text{-}Br)\}(\mu_2\text{-}\mathbf{L1})]_n$ (**CP2**) was isolated upon treatment of CuBr with **L1** in MeCN solution. Likewise, treatment of **L1** with CuCl in a 1:1 ratio results in formation of the unusual 1D CP $[\{Cu(\mu_2\text{-}Cl)\}(\mu_2\text{-}\mathbf{L1})]_n$ (**CP3**). In contrast to **CP1** incorporating dinuclear $Cu(\mu_2\text{-}I)_2Cu$ units as connection nodes, the isolated Cu atoms of **CP2** and **CP3** are bridged by a single μ_2-Br or μ_2-Cl ligand giving rise to infinite $[Cu(\mu_2\text{-}X)Cu]_n$ ribbons. Reaction of ferrocenecarbaldehyde with 1,2-ethanedithiol affords the crystallographically characterized ferrocenyl-dithiolane $Fc\text{-}C(H)S_2C_2H_4$ (**L2**). **L2** was used as organometallic dithioether ligand to assemble, upon treatment with CuI, the original luminescent 1D CP $[\{Cu_2(\mu_4\text{-}I)(\mu_2\text{-}I)\}(\mu_2\text{-}\mathbf{L2})]_n$ (**CP4**), in which both S atoms of one **L2** molecule span two copper centers of a meander-shaped infinite $(CuI)_n$ ribbon. Upon reaction of **L2** with CuBr in a 1:2 ratio, the discrete tetranuclear cluster $[\{Cu_4(\mu_2\text{-}Br)_2(\mu_3\text{-}Br)_2\}(\mu_2\text{-}\mathbf{L2})_2(MeCN)_2]$ (**CL1**) is formed.

Keywords Copper halide cluster • coordination polymer • 1,3-dithiolane • ferrocene • thioether.

1 Introduction

The five-membered heterocyclic ligand tetrahydrothiophene (THT) is known to form a great variety of molecular complexes and coordination polymers (CPs) with various transition metals [1-4]. Notably, for the soft coinage metal ions Cu, Ag and Au(I), numerous structurally characterized examples coordinated by terminal or bridging THT ligands are documented [5-11]. Even mixed-valence Cu(I)-Cu(II) compounds such as polymeric penta-μ-chloro-tris-μ-tetrahydrothiophene-tetracopper(I,II) have been prepared [12]. In the case of the five-membered heterocycle 1,2-dithiolane, in which one CH_2-unit is replaced by a second sulfur atom, there is one report on its coordination to $Hg_2(NO_3)_2$ yielding the Hg(I) adduct 1,2-dithiolane • $Hg_2(NO_3)_2$. Furthermore, the dinuclear organometallic species [μ_2-1,2-dithiolane)-bis(η^5-cyclopentadienyl)-dicarbonyl-manganese] has been crystallographically characterized [13,14]. The fluxional complexes [$M(CO)_5$(1,3-dithiolane)] (M = Cr, Mo, W) ligated by the isomeric heterocycle 1,3-dithiolane (1,3-dithiacyclopentane) have been investigated by NMR spectroscopy [15, 16]. But surprisingly, a survey of the CSD Database revealed that up to date, no transition metal complex ligated by this thiaheterocycle has been structurally characterized. The only related compound is the polymeric material $[Ag(NO_3)(C_4H_8OS_2)]_n$, in which 1,3-dithiolane-2-methanol is bound to $AgNO_3$ through dative Ag-S bonds and additional supramolecular hydrogen interactions [17].

In the context of our on-going study on the assembly of CPs and MOFs by reaction of aromatic and aliphatic dithioethers $RS(CH_2)_nSR$ (n = 1-8) with CuX salt (X = I, Br, Cl), we have described in series of papers the construction and structural features of numerous molecular clusters and coordination networks, with dimensionalities varying from 0D-3D [18-25]. The occurrence of polynuclear $(CuX)_n$ clusters as secondary building units (SBUs) often confers these materials, notably in the case of $(CuI)_n$ SBUs, interesting luminescence properties [26].

We have now extended our investigation on the coordination of the simple cyclic dithioether 1,3-dithiolane **L1**, in which the two potential *S*-donor sites are separated by one methylene unit and present our results concerning the coordination of 1,3-dithiolane on Cu(I) salts. This project is in part motivated as comparative study with respect to our

previous work on the coordination chemistry of the open-chain dithioether analogues RS-CH_2-SR [24, 25] and in part to fill the gap between the versatile coordination chemistry of THT (see above) and the almost unexplored coordination chemistry of 1,3-dithiolane. As entry in the design of organometallic materials, we have furthermore synthesized the hitherto unknown ferrocenyl-functionalized derivative [1,3-Fc-C(H)S_2(CH_2)$_2$] **L2**, whose coordination on CuI and CuBr has been investigated.

2 Results and Discussion

2.1 Synthesis and crystallographic characterization of [Cu(μ_2-I)$_2$Cu}(μ_2-**L1**)$_2$]$_n$ (CP1)

Upon treatment of a solution of CuI in MeCN with a slight excess of 1,3-dithiolane, rapidly the precipitation of a microcrystalline colorless product started, which was formed in almost quantitative yield and analyzed as [Cu(μ_2-I)$_2$Cu}(μ_2-**L1**)$_2$]$_n$ (**CP1**) (Scheme 1).

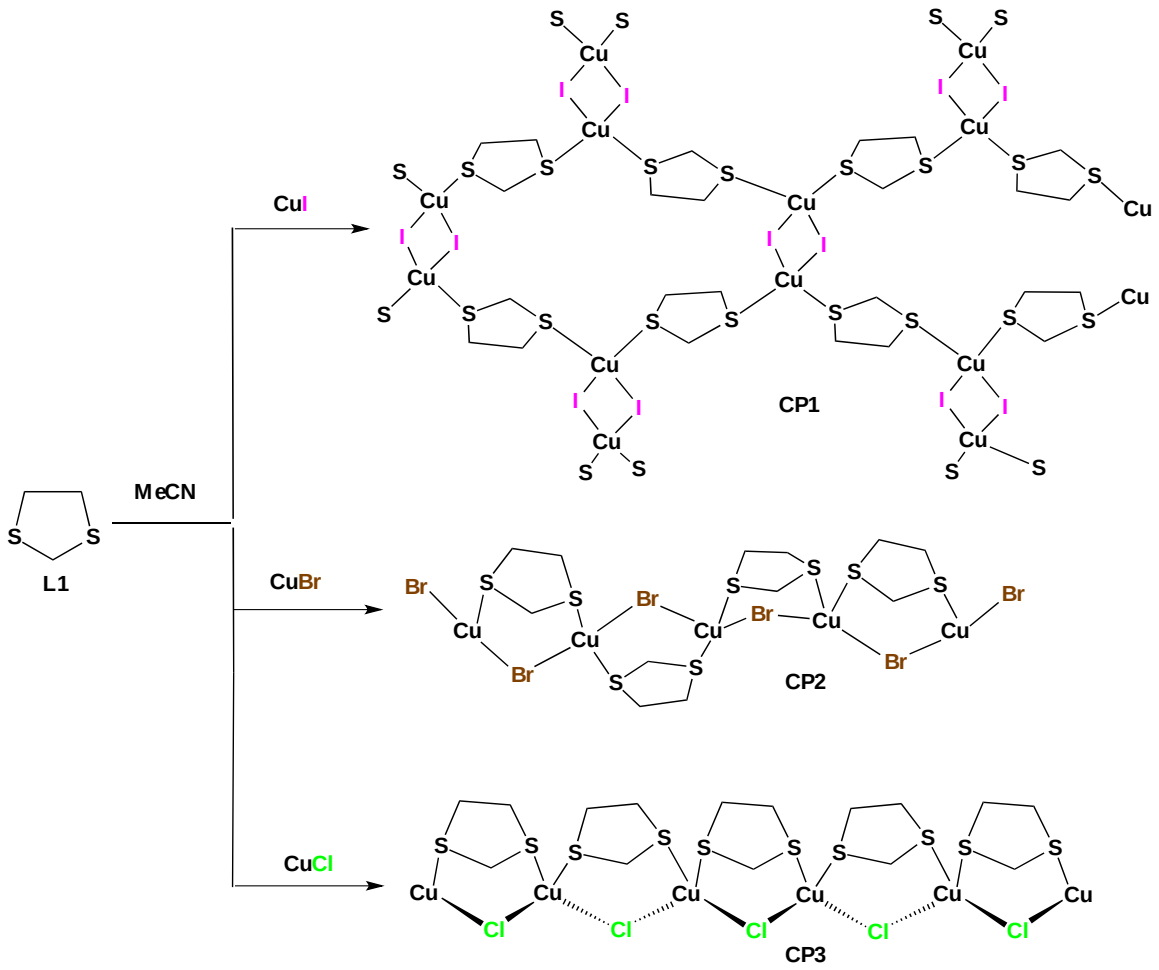

Scheme 1 Synthesis of $[\{Cu(\mu_2\text{-}I)_2Cu\}(\mu_2\text{-}\mathbf{L1})_2]_n$ (**CP1**), $[\{Cu(\mu_2\text{-}Br)\}(\mu_2\text{-}\mathbf{L1})]_n$ (**CP2**), and $[\{Cu(\mu_2\text{-}Cl)(\mu_2\text{-}\mathbf{L1})]_n$ (**CP3**)

Since this compound is only sparingly soluble in MeCN even under reflux, we dissolved a small amount in refluxing EtCN and succeeded to grow suitable single-crystals for an X-ray diffraction study (Table 1). As shown in Fig. 1, a 2D network has been generated, in which both sulfur atoms of **L1** span two adjacent $Cu(\mu_2\text{-}I)_2Cu$ rhomboids, thus forming 20-membered macrocycles in the layer. Similar 2D grids have been obtained previously by reaction of CuI with the open-chain dithioethers 1,3-bis(phenylthio)propane and 1,3-bis(phenylthio)ethane yielding $[\{Cu(\mu_2\text{-}I)_2Cu\}_2\{\mu\text{-}PhS(CH_2)_3SPh\}_2]_n$ and $[\{Cu(\mu_2\text{-}I)_2Cu\}_2\{\mu\text{-}PhS(CH_2)_2SPh\}_2]_n$, respectively [18, 22].

In these centrosymmetric SBUs, the Cu···Cu separation is of 2.9081(7) Å at 294 K, excluding any cuprophilic interaction [27-29]. After recording the structure at 100 K, the

Cu···Cu separation shrinks to 2.8743(5) Å, but remains above the sum of the Van der Waals radii of two Cu atoms (2.8 Å). No phase transition was observed in this temperature interval, the space group remaining P2(1)/n. A literature survey reveals that in $Cu_2I_2S_4$ complexes, the Cu····Cu separation is quite variable. An example in the short range is given by a dithioether-functionalized tetrathiafulvalene complex and $[(THT)_2Cu(\mu\text{-}I)_2Cu(THT)]_2$ with separations of only 2.6469(15) and 2.675 Å, respectively. But much longer Cu···Cu separations of 3.0089(15) Å and even 3.18 Å have been reported for the 1D polymer $[\{Cu(\mu_2\text{-}I)_2Cu\}\{\mu\text{-}PhS(CH_2)_5SPh\}_2]_n$ [22] and the 2D material $[(Cu_2I_2(dtpcp)_2]\bullet thf)]_n$ (dtpcp = 2,11-dithia[3.3]paracyclophane) [30], respectively. Each Cu atom exhibits a distorted tetrahedral environment, coordinated by two bridging iodide ligands and two S atoms stemming from two distinct **L1** ligands.

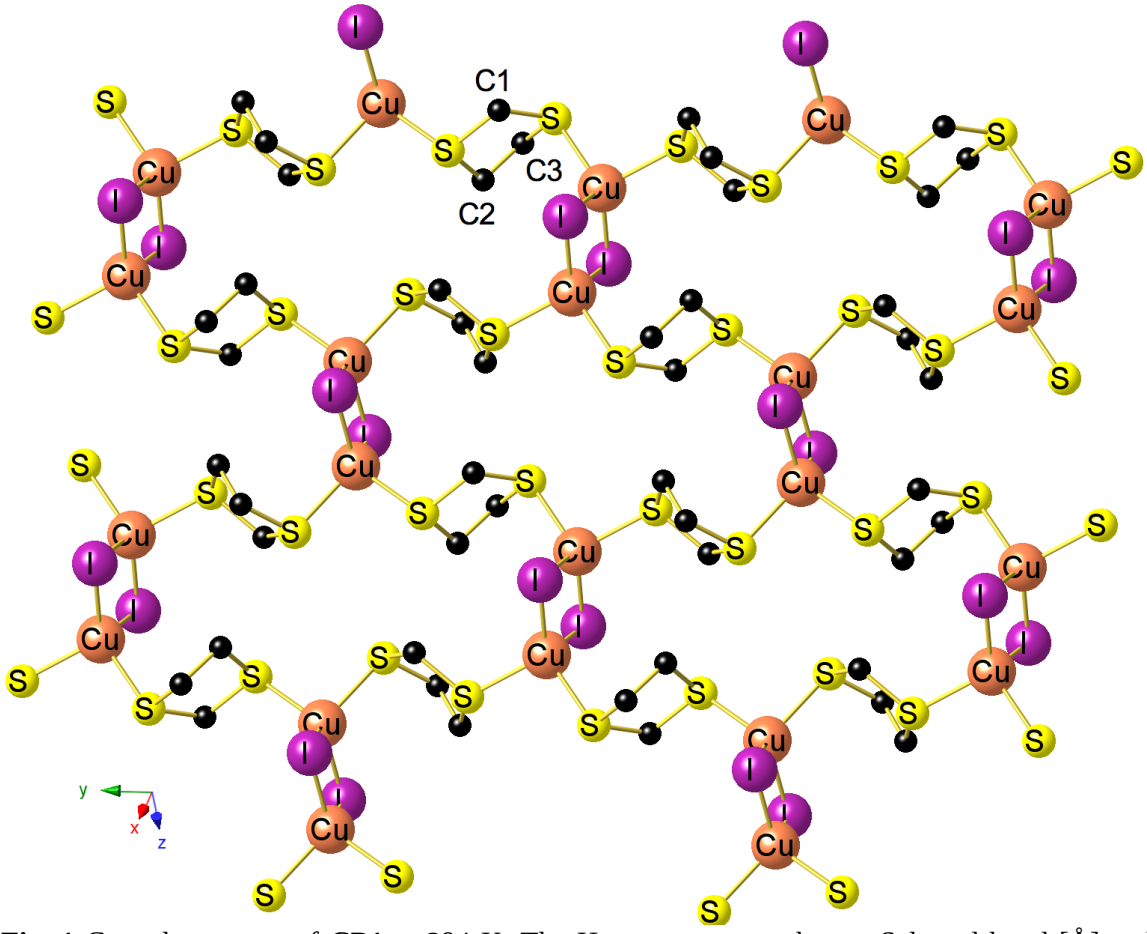

Fig. 1 Crystal structure of **CP1** at 294 K. The H atoms are not shown. Selected bond [Å] and angles [°]: Cu···Cu[1] 2.9081(7), Cu–I 2.6200(6), Cu–I[1] 2.6219(6), Cu–S1[2] 2.3716(6), Cu–S2

2.3497(6), C1–S1 1.8042(18), C1–S2 1.8179(18), C3–S2 1.811(2), C2–C3 1.506(3), Cu–I–Cu[1] 67.392(13), I–Cu–I[1] 112.609(13), S1[2]–Cu–S2 96.16(2), S1[2]–Cu–I 109.978(19), S1[2]–Cu–I[1] 112.764(17), S2–Cu–I[1] 108.081(16), S2–Cu–I 116.246(17). Symmetry transformations used to generate equivalent atoms: [1]1-X, 1-Y, -Z; [2]3/2-X, -1/2+Y, 1/2-Z; [3]3/2-X, 1/2+Y, 1/2-Z.

Using the CrystalMaker Software (version 8.7.6), the porosity (corrected for first-nearest-neighbor sphere overlap and site visibility) of **CP1** has been determined. At 293 K the unit cell volume is 699.156 Å^3, the filled space is 194.400 Å^3 (27.81%) and the void space amounts to 504.756 Å^3 (72.19%) per unit cell. The purity of the phase was checked by recording the PXRD spectrum. The comparison of the experimental spectrum with the simulated one ascertained the homogeneity of the isolated product (Fig. 2).

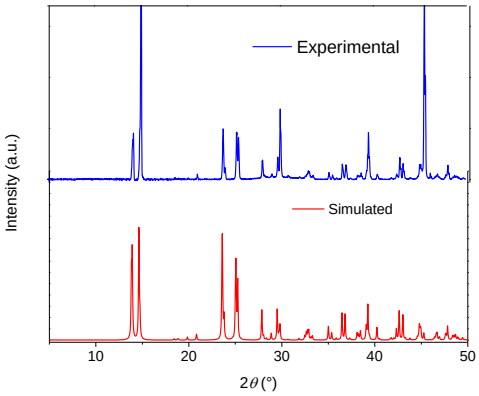

Fig. 2 Experimental PXRD pattern (top) and simulated spectrum (bottom) of **CP1**

2.2 Synthesis and Crystallographic Characterization of [{Cu(μ_2-Br)}(μ-L1)]$_n$ (CP2) and [{Cu(μ_2-Cl)}(μ-L1)]$_n$ (CP3)

In 1985, Ainscough and Brodie mentioned briefly that the reduction of methanolic solutions of $CuCl_2 \cdot 2\ H_2O$ or $CuBr_2$ by H_3PO_2 and subsequent addition of 1,3-dithiolane to the solution yield white precipitates, whose elemental analyses indicated formation of 1:1 adducts of composition [CuX(1,3-dithiolane] (X = Cl, Br), but no further characterization information was provided [12]. In an alternative approach, we reacted as described above for the synthesis of **CP1**, CuBr in MeCN solution with a slight excess of **L1** and isolated in high yield a colorless microcrystalline solid. Elemental analyses

indicated formation of 1:1 adduct of composition [CuBr(**L1**)] in line with the paper of Ainscough and Brodie [12]. Like **CP1**, this compound is air-stable for short periods, but an unpleasant faint smell of 1,3-dithiolane is indicative of slow dissociation of volatile **L1**. By slow evaporation of a concentrated MeCN solution fine needle-shaped crystals could be grown, which were suitable for a single-crystal X-ray diffraction study. The crystal structure shown in Fig. 3 confirms the 1:1 copper-to-ligand ratio of 1D polymeric $[\{Cu(\mu_2\text{-}Br)\}(\mu_2\text{-}\mathbf{L1})]_n$ (**CP2**). The structural arrangement is quite different from that of **CP1** and concerns not only the dimensionality, but also the connectivity of the Cu atoms within the ribbon. These are not associated in form of rhomboid $Cu(\mu_2\text{-}Br)Cu$ dimers, as encountered in the 1D CPs $[\{Cu(\mu_2\text{-}Br)_2Cu\}\{\mu_2\text{-}ArSCH_2SPh\}_2]_n$ and $[\{Cu(\mu_2\text{-}Br)_2Cu\}\{\mu_2\text{-}ArS(CH_2)_5SAr\}_2]_n$ (Ar = Ph, *p*-Anisyl, *p*-Tol) [22, 24], but as isolated Cu atoms interconnected via a single μ_2-halide ligand. Within the infinite Cu–Br–Cu–Br–Cu–Br array, the copper atoms are not symmetry-related and quite distant relative to their neighbors with Cu1⋯Cu2, Cu2⋯Cu3 and Cu1⋯Cu3 separations of 3.485, 3.547 and 3.700 Å, respectively. In consequence, there are also three non-equivalent μ_2-bromo ligands, whose Cu–Br distances and Cu–Br–Cu angles are listed in the caption of Fig. 3. To the best of our knowledge, **CP2** exhibits a hitherto unknown structural arrangement encountered in thioether-assembled Cu(I) CPs.

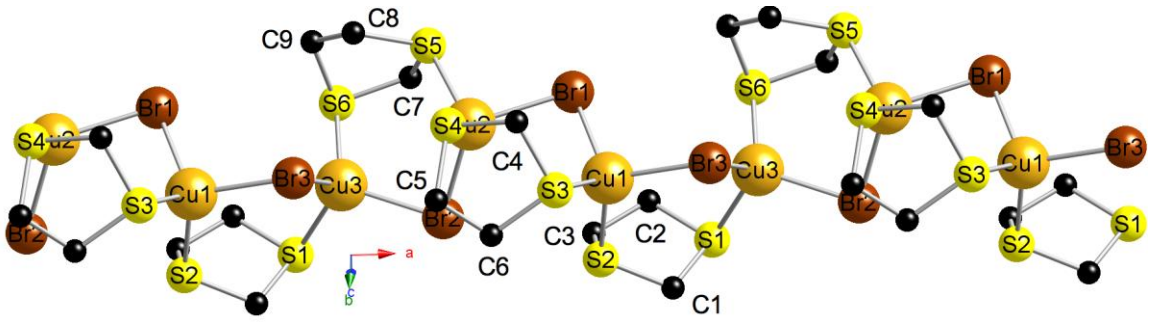

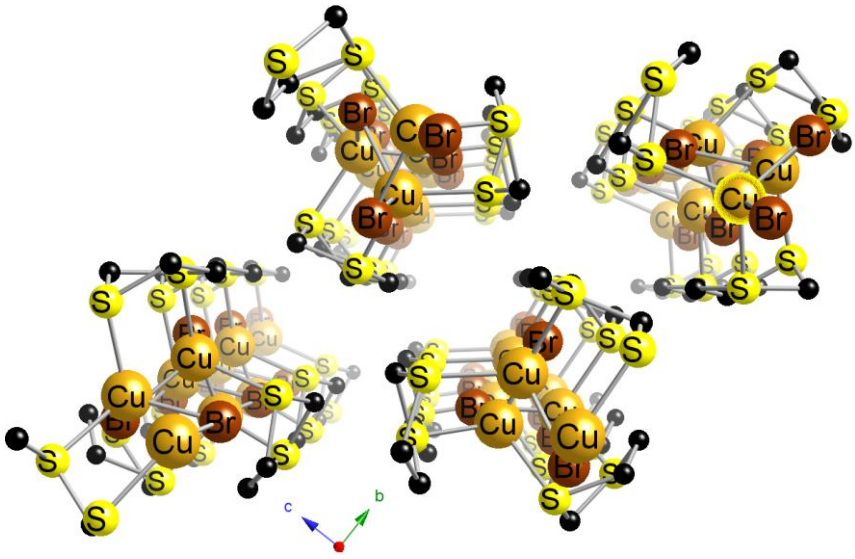

Fig. 3 *Top:* Crystal structure of **CP2** running along the *a* axis. The H atoms are not shown. Selected bond [Å] and angles [°]: Cu1–Br1 2.4343(4), Cu2–Br1 2.5009(4), Cu2–Br2 2.4740(4), Cu3–Br2 2.4692(4), Cu1^{1}–Br3 2.4926(4), Cu3–Br3 2.4392(4), Cu1–Br3^{2} 2.4926(4), Cu1–S2 2.2967(6), Cu1–S3 2.3379(6), Cu2–S4 2.2853(6), Cu2–S5 2.3467(6), Cu3–S1^{1} 2.3511(6), Cu3–S6 2.3103(6); Cu1–Br1–Cu2 89.850(12), Cu3–Br2–Cu2 91.691(12), Cu3–Br3–Cu1^{1} 97.210(12), Br1–Cu1–Br3^{2} 110.141(13), S2–Cu1–Br1 110.334(18), S2–Cu1–Br3^{2} 111.738(18), S2–Cu1–S3 111.88(2), Br2–Cu2–Br1 115.305(14), S4–Cu2–S5 114.36(2), S4–Cu2–Br1 110.70(2) S4–Cu2–Br2 110.63(2), S5–Cu2–Br1 95.011(18), Br3–Cu3–Br2 109.167(13), S6–Cu3–Br2 111.536(19), S6–Cu3–Br3 116.385, S6–Cu3–S1^{1} 100.84(2). *Bottom:* Perspective view of four chains of **CP2** running down the *a* axis.

A colorless microcrystalline solid of composition [CuCl(**L1**)] could also be isolated in over 85% yield after mixing a MeCN solution of CuCl with **L1**. X-ray suitable crystals of [CuCl(**L1**)] crystalizing in the monoclinic space group *Cc* were grown from hot EtCN. The structure determination revealed formation of a 1D CP [{Cu(μ_2-Cl)}(μ-**L1**)]$_n$ (**CP3**), which is illustrated in Figure 4. The most salient feature of this structure is the unusual alignment of the CuCl units, which in contrast to **CP1** are bridged only by a single μ_2-halide ligand. Another rare example of a 1D CP constructed by CuCl is [(THT)$_3${Cu$_2$(μ_2-Cl)$_2$}]$_n$, but the latter contains distinct Cu(μ_2-Cl)Cu rhomboids [7]. We are also aware of a CP [(Cu(μ_2-Cl)Cu)}(η-oxathietane)]$_n$ containing a somewhat similar inorganic CuCl

ribbon. However, in this Cu(II) compound, the stepped chain is constituted of doubly-bridge $CuCl_2$ units ligated via the *S*-donor site of 1,4-oxathietane [30].

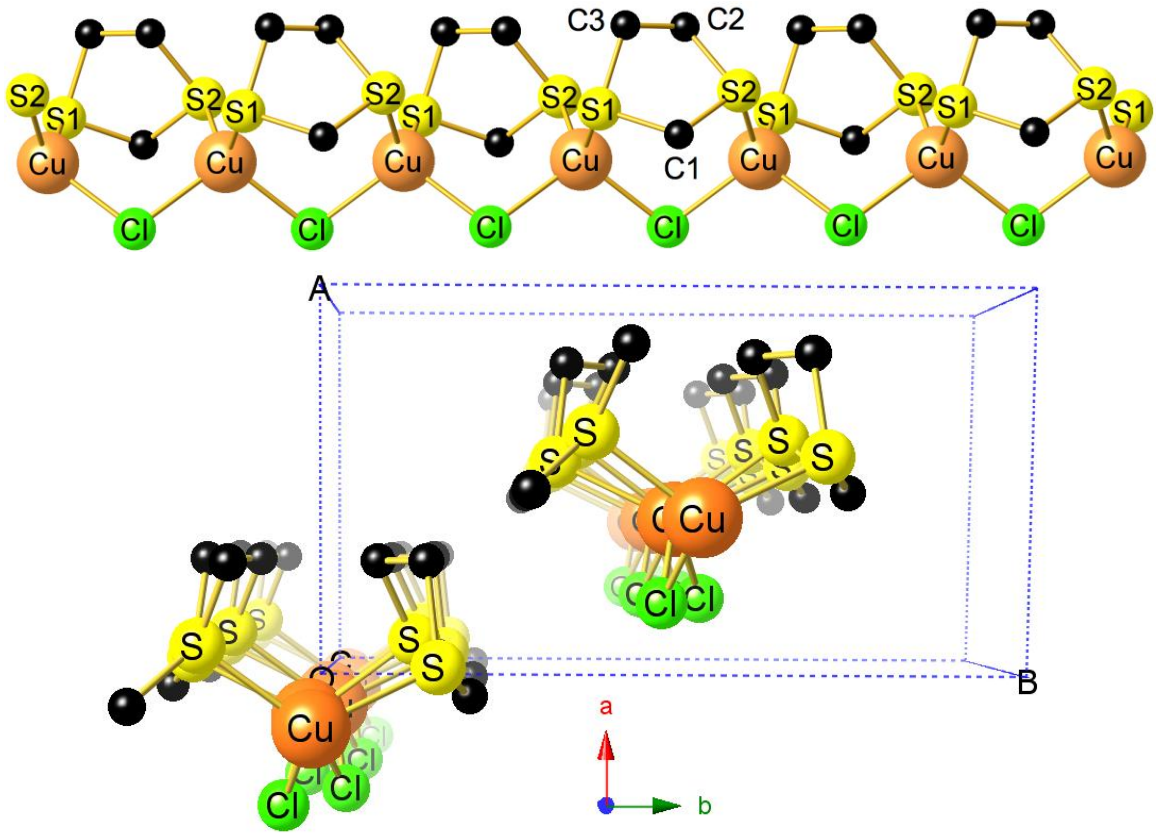

Fig. 4 *Top:* Crystal structure of **CP3** running along the *c* axis. The H atoms are not shown. Selected bond [Å] and angles [°]: Cu–Cl 2.3315(6), Cu–Cl^1 2.3649(6), Cu–S1 2.2911(7), Cu–$S2^1$ 2.3050(7); Cu–Cl–Cu^2 103.40(3), Cl–Cu–Cl^1 107.20(3), S1–Cu–$S2^1$ 118.50(2), S1–Cu–Cl 110.40(3), S1–Cu–Cl^1 105.12(3), $S2^1$–Cu–Cl^1 107.44(2), S2–C1–S1 108.53(13). Symmetry transformations used to generate equivalent atoms: ^{1}+X, 1-Y, -1/2+Z; ^{2}+X, 1-Y, 1/2+Z *Bottom:* Perspective view of two chains of **CP3** running down the *c* axis.

At the first glance, there is some resemblance between the one-dimensional ribbons of **CP2** and **CP3**. But **CP3** is more symmetric than its bromo-counterpart incorporating a single type of copper atoms and μ_2-chloro bridges. Within the chain, each Cu(I) center is tetrahedrally surrounded by two Cl and two S atoms stemming from two adjacent **L1** ligands. The separation between each individual Cu atom of 3.686 Å is far too long to contribute to any bonding interaction. The mean Cu–Cl bond length (2.3482(6) Å) of the

almost symmetrically bridging μ_2-Cl atom matches roughly with those of [{$Cu_2(\mu_2$-$Cl)_2$}$(THT)_3]_n$ [(2.330(2) and 2.404(3) Å] and of 2D polymeric [{$Cu_2(\mu_2$-$Cl)_2$}$(Me_2S)_2]_n$ [(2.334(1) and 2.359(1) Å]. As shown in Fig. 4 (see below), the chloro ligands are not aligned in a parallel and eclipsed manner with respect to the Cu····Cu····Cu axis, but staggered with a Cu–Cl–Cu–Cl torsion angle of 151°. The only other example of a CP exhibiting the same structural features as encountered for **CP3** is [{Cu(μ_2-Cl)}(μ-lipoic acid)]$_n$, where α-lipoic acid is coordinating to the Cu atom via its cyclic disulfide group and bridges two adjacent copper centers [32]. Five-membered rings of the type Cu–Cl–Cu–S–S– are building blocks in this 1D polymer. Note that the Cu····Cu separations of 3.559 Å are somewhat shorter than those of **CP3** (3.559 *vs*. 3.686 Å), whereas the mean Cu–S and Cu–Cl bond lengths are comparable [32].

2.3 Synthesis and Structural Characterization of Ferrocenyl-dithiolane L2

Due to the chemical stability associated with the electrochemical redox-activity of a ferrocenyl fragment, numerous organometallic polymers bearing a ferrocenyl-unit in the main chain or as pendant side-fragment have been described in the literature [33, 34]. We have previously described the synthesis and coordination chemistry of thioether-functionalized vinyl-ferrocenes [35]. An alternative facile access to thioether-functionalized ferrocenes is the acid-catalyzed conversion of ferrocenecarbaldehyde with 1,2-ethanedithiol yielding the cyclic thioacetal **L2** (Scheme 2).

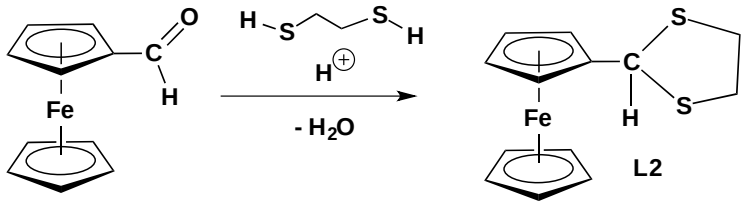

Scheme 2 Synthesis of the cyclic ferrocenyl-dithioacetal **L2**

This stable orange compound is well soluble in aromatic and halogenated solvents and was recrystallized from toluene/hexane. The NMR data are presented in the experimental section; the molecular structure is shown in Fig. 5 and deserves no special comment.

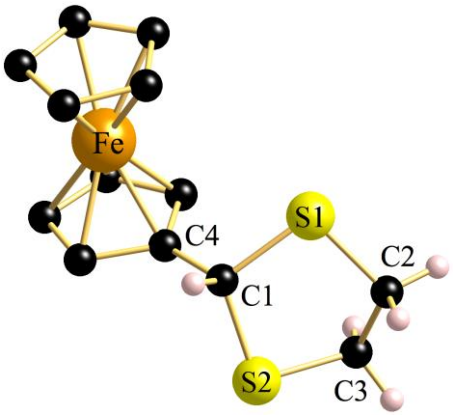

Fig. 5. Molecular structure of **L2**. Selected bond lengths (Å) and angles (°): C1–S1 1.832(2), C1–S2 1.830(2), C2–S2 1.809(2), C3–S1 1.806(2), C2–C3 1.509(3), C4–C1 1.493(3); C3–C2–S2 107.74(14), C3–C2–S2 107.74(14), S2–C1–S1 108.50(9), C3–S1–C1 96.50(9), C1–S2–C2 98.11(9), S2–C1–C4 112.05(14), C4–C1–S1 112.84(14).

2.4 Reaction of Ferrocenyl-dithiolane L2 with CuI and CuBr

With **L2** in hands, we extended our investigation on the complexation of this organometallic ligand to CuI. Upon addition of 2 equivalents of a CuI solution in MeCN with **L2** at ambient temperature, formation of an orange precipitate **CP4** was noticed (Scheme 3). The outcome of the reaction is insensitive to the metal-to-ligand ratio, since conducting the reaction with 4 equivalents of CuI yielded again **CP4**, as checked by comparison of the PXRD spectra (Fig. 7). By re-dissolution in refluxing MeCN, X-ray suitable crystals crystallizing in the monoclinic space group P2(1)/c were grown.

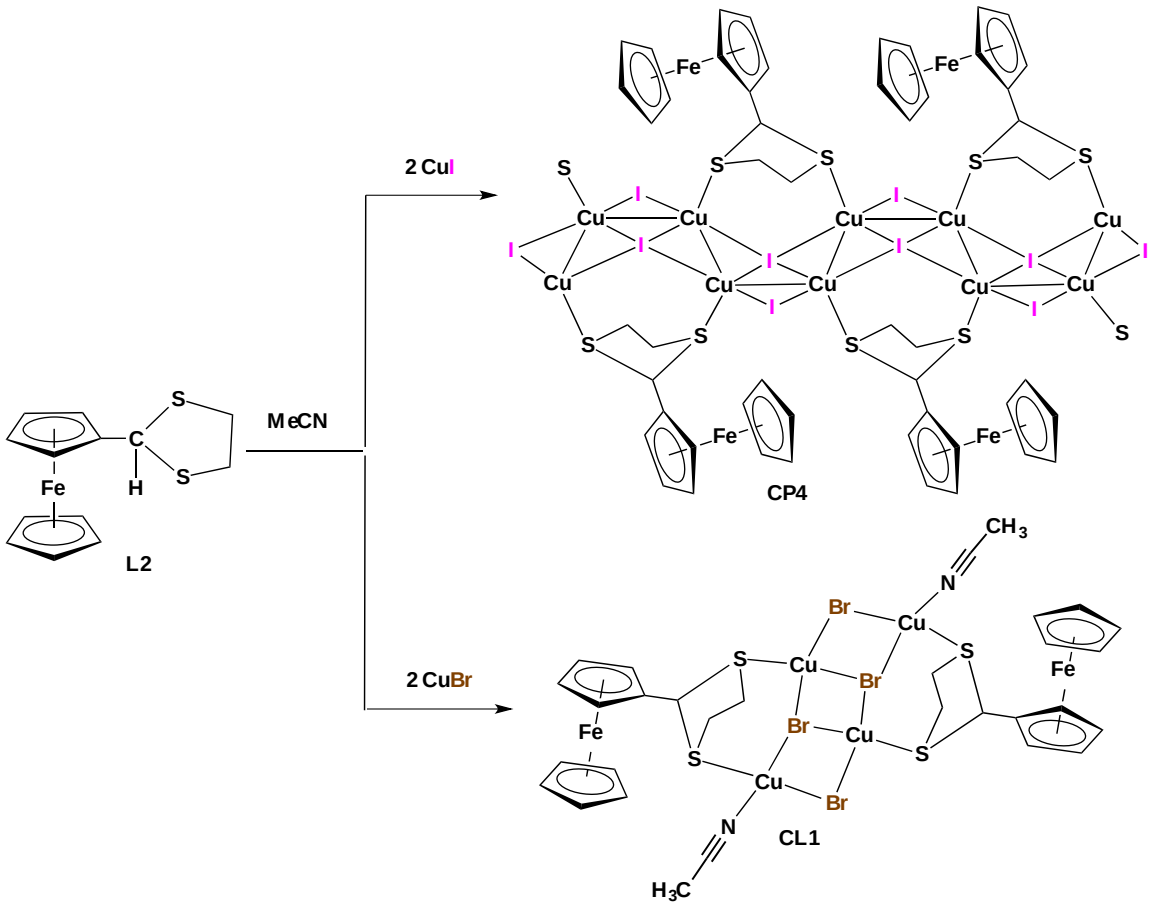

Scheme 3 Synthesis of the organometallic 1D polymer **CP4** and the 0D molecular cluster **CL1**

The structure of this orange-colored air-stable product $[\{Cu_2(\mu_4\text{-I})(\mu_2\text{-I})\}(\mu_2\text{-}\mathbf{L2})]_n$ **(CP4)** is shown in Fig. 6. The inorganic CuI ribbon of this 1D material can be described as infinite meander-shaped $(Cu1–Cu1\cdots Cu2–Cu2\cdots Cu1–Cu1)_n$ array, were Cu1–Cu1 blocks (d = 2.7373(10) Å) are interconnected to Cu2–Cu2 blocks (d = 2.8307(11) Å) through somewhat looser Cu1···Cu2 contacts of 2.8733(8) Å. The latter are quite symmetrically μ_2-bridged by a I2 atom with Cu1–I2 distances of 2.5807(6) and Cu2–I2 2.5907(6) Å. Furthermore, each Cu1–Cu1···Cu2–Cu2 meander unit is capped by a μ_4-bridging I1 atom. There are some few examples of discrete polynuclear CuI compounds ligated by *P*- or *N*-donor sets featuring both μ_2- and μ_4-I ligands [36-38], but we are not aware of any thioether-based CP displaying this unique arrangement. The two sulfur atoms of **L2** span additionally two remote Cu1 and Cu2 atoms with Cu1–S1 and Cu2–S2 bond lengths of 2.3053(11) and 2.3131(11) Å, respectively.

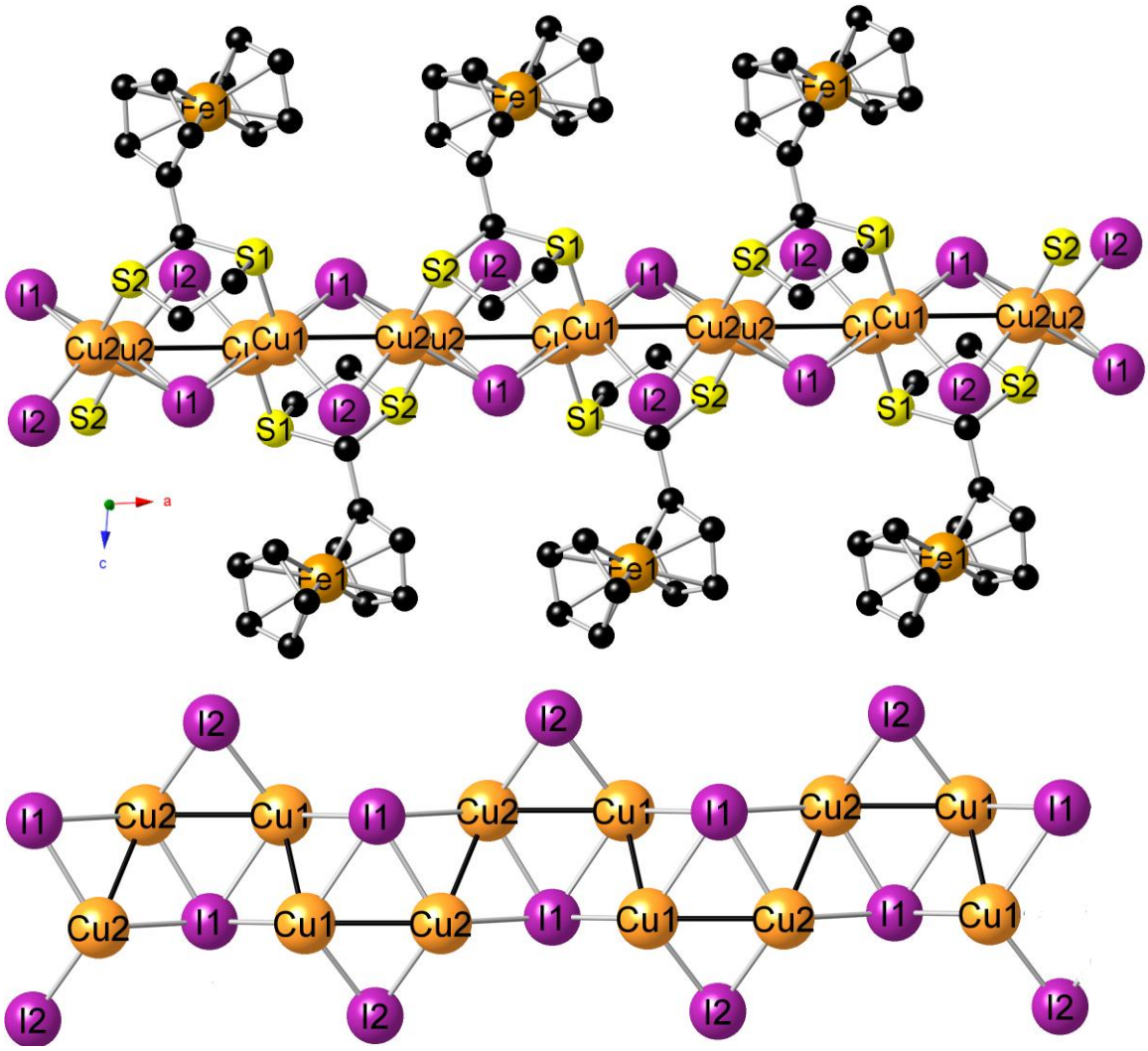

Fig. 6. *Top:* View of the 1D ribbon of $[\{Cu_2(\mu_4\text{-I})(\mu_2\text{-I})\}(\mu\text{-}\mathbf{L2})]_n$ **(CP4)** running along the *a* axis in the crystal. Selected bond lengths (Å) and angles (°): Cu1–Cu1^1 2.7373(10), Cu1–Cu2 2.8733(8), Cu2–Cu2^2 2.8307(11), Cu1–I1 2.7340(6), Cu1^1–I1 2.6883(6), Cu2–I1 2.6323(6), Cu2^1–I1 2.7115(6), Cu1–I2 2.5807(6), Cu2–I2 2.5907(6), Cu1–I1^1 2.6883(6), Cu1–S1 2.3053(11), Cu2–I1^2 2.7115(6), Cu2–S2^3 2.3131(11); Cu1–I1–Cu1^1 60.63(2), Cu1^1–I1–Cu2^2 108.390(19), Cu2^2–I1–Cu1 116.845(18), Cu2–I1–Cu1^1 110.567(19), Cu1–I1–Cu2 64.714(18), Cu2–I1–Cu2^2 63.95(2), Cu1–I2–Cu2 67.505(19), I1–Cu1–I1^1 119.37(2), I1–Cu1–Cu1^1 58.86(2), I1–Cu1–Cu2 55.929(15), I2–Cu1–Cu2 56.412(16), Cu1^1–Cu1–Cu2 102.41(3), S1–Cu1–Cu2 105.76(3), I1–Cu2–Cu1 59.357(16), I1–Cu2–Cu2^2 59.385(19), I2–Cu2–Cu1 56.083(16), S2^3–Cu2–Cu1 111.07(3). *Bottom:* View of the meander-shaped inorganic Cu1–Cu1···Cu2–Cu2 array spanned by μ_2-I and μ_4-I atoms.

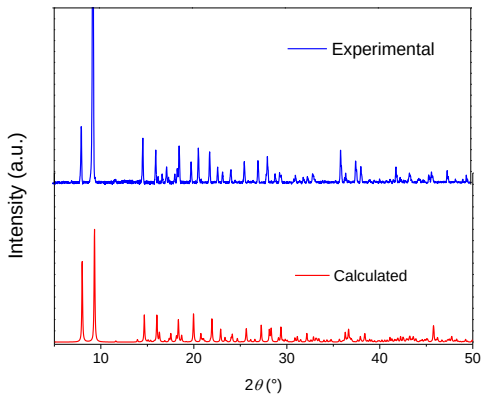

Fig. 7 Experimental PXRD pattern (top) and simulated spectrum (bottom) of **CP4**

The impact of the nature of the halide ligand on the outcome of the reaction is demonstrated by the fact that reaction of **L2** with CuBr under identical reaction conditions yields exclusively the molecular cluster [{$Cu_4(\mu_2\text{-}Br)_2(\mu_3\text{-}Br)_2$}(μ-**L2**)$_2$(MeCN)$_2$] (**CL1**). Although this orange compound is quite stable, transparent crystal of **CL1** become opaque after exposure to air, probably due to slow loss of copper-bound MeCN. This was confirmed by the absence of coordinated MeCN molecules in the IR spectra. The molecular structure shown in Fig. 8 reveals that the tetranuclear core motif of **CL1** consists of a central Cu-Cu dimer [*d*(Cu1⋯Cu1^1 2.8061(7) Å), on which are condensed two additional CuBr units [*d*(Cu1⋯Cu2 3.089(4) Å), each bearing a MeCN ligand. This step-like structural core motif, also called open cubane (in contrast to the isomeric closed $Cu_4(\mu_3\text{-}Br)_4$ cubane cluster) is known for $Cu_4(\mu\text{-}Br)_4(PPh_3)_4$ bearing two μ_2- and two μ_3-bromo ligands [39, 40]. Other examples are with nitrogen bases [Cu_4Br_4(2-dpmpy)$_4$] (2-dpmpy = 2-(diphenylmethyl)pyridine) and [Cu_4Br_4(1,2,3-triazq)$_2$] (1,2,3-triazq = [1,2,3]triazolo[1,5-**a**]quinolone) [41, 42].

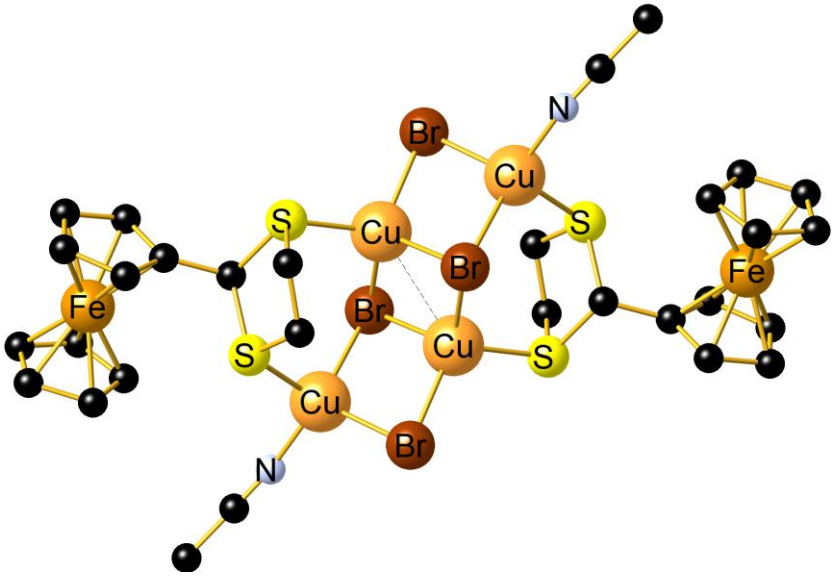

Fig. 8 Molecular structure of [{$Cu_4(\mu_2\text{-}Br)_2(\mu_3\text{-}Br)_2$}($\mu$-**L2**)$_2$(MeCN)$_2$] (**CL1**) Selected bond lengths (Å) and angles (°): Cu1···Cu1^1 2.8601(7), Cu1–Br1 2.4454(4), Cu2^1–Br1 2.4603(5), Cu1^1–Br2 2.5572(5), Cu1–Br2 2.5127(4), Cu2–Br2 2.5435(4), Cu1–Br2^1 2.5573(5), Cu2–Br1^1 2.4602(5), Cu1–S1 2.2760(8), Cu2–S2 2.3183(8), Cu2–N1 1.990(3); Cu1–Br1–Cu2^1 78.058(14), Cu1–Br2–Cu1^1 68.678(15), Cu1–Br2–Cu2 99.958(14), Cu2–Br2–Cu1^1 74.547(13), Br1–Cu1–Br2 110.917(16), Br1–Cu1–Br2^1 102.614(15), Br1–Cu1–Cu1^1 120.59(2), Br2–Cu1–Br2^1 111.320(15), Br2–Cu1–Cu1^1 56.398(13), S1–Cu1–Br1 113.23(2), S1–Cu1–Br2^1 109.76(2), S1–Cu1–Br2 108.91(2), S1–Cu1–Cu1^1 125.95(3), Br1^1–Cu2–Br2 102.594(16), S2–Cu2–Br1^1 109.82(2), S2–Cu2–Br2 105.05(2), N1–Cu2–Br1^1 111.43(7), N1–Cu2–Br2 122.51(7), N1–Cu2–S2 104.99(8). Symmetry transformations used to generate equivalent atoms: ^{1}+X, 1/2-Y, +Z; ^{2}+X, 3/2-Y,+Z; ^{3}2-X, 1-Y,1-Z.

A molecular architecture very similar to that of **CL1** has been recently reported for [$Cu_4Br_4(L)_2(MeCN)_2$] (L = 3,7-di(3-pyridyl)-1,5-dioxa-3,7-diazacyclooctane) [43]. Like in the latter compound, four Cu atoms and four Br atoms form a step-like or stair-like [Cu_4Br_4] cluster core with each of the two MeCN molecules ligated at each end of the stair with a Cu–N bond length of 1.990(3) Å. Each Cu2 center is tetrahedrally coordinated by one S atom from **L2**, one μ_2-Br atom, one μ_3-Br atom and a N atom from the MeCN molecule. The coordination sphere around Cu1 consists of one S atom from **L2**, one μ_2-Br atom and two μ_3-Br atoms. The two S atoms of **L2** span Cu1 and Cu2 forming a six-membered ring. We have recently described a 2D coordination polymer

$[(Cu_3Br_3)(MeSEt)_3]_n$ where each layer is constructed from alternating rhomboid Cu_2Br_2 dimers and open stepped-cubane Cu_4Br_4 units, which are linked through two μ_2-MeSEt ligands [44]. However, **CL1** seems to be the first molecular compound exhibiting a step-like $Cu_4(\mu_2\text{-}Br)_2(\mu_3\text{-}Br)_2$ core ligated with a mixed *S/N* donor set.

2.5 Luminescence Properties of CP1 and CP4

Di- and polynuclear CuI compounds coordinated by *N*-, *P*- and *S*-donor ligands exhibit often intense luminescence and interesting photophysical properties [45-51]. We therefore recorded the solid-state luminescence spectrum of **CP1,** which exhibits the main emission at 440 nm along with a shoulder at lower energy at about 558 nm. The luminescence is only of medium intensity, a feature observed for other CuI • thioether compounds incorporating a dinuclear $Cu(\mu_2\text{-}I)_2Cu$ rhomboid instead of higher-nuclear $(CuI)_n$ (n = 4, 6, 8) motif [18, 22, 47]. In the case of **CP1**, the loose Cu···Cu contact of 2.9081(7) Å may further contribute to the relative weakness of the emission.

For **CP4**, the luminescence spectrum looks much alike that of **CP1** with the exception that the band located at 558 nm is of higher intensity. The low-energy band may be tentatively assigned to a cluster-center excited state (CC*), whereas that found at higher energy corresponds to a M/XLCT (metal/halide-to-ligand charge transfer) excited state. The fact that **CP4** exhibits a more intense second band at lowest energy is in accordance with the shorter Cu···Cu distances found in this material compared to **CP1**. In contrast to the well-explored photophysical properties of $Cu_4I_4L_4$ clusters of the closed-cubane type, [46, 48, 49, 51] those of 1D $(CuI)_n$ ribbons have been scarcely investigated. Therefore, in the absence of more advanced photophysical investigations a concise discussion on the photophysics of **CP4** and an eventual quenching effect caused by the ferrocenyl-fragment remains speculative. In contrast to **CP1** and **CP4**, the CuBr- and CuCl-containing materials exhibited no luminescence.

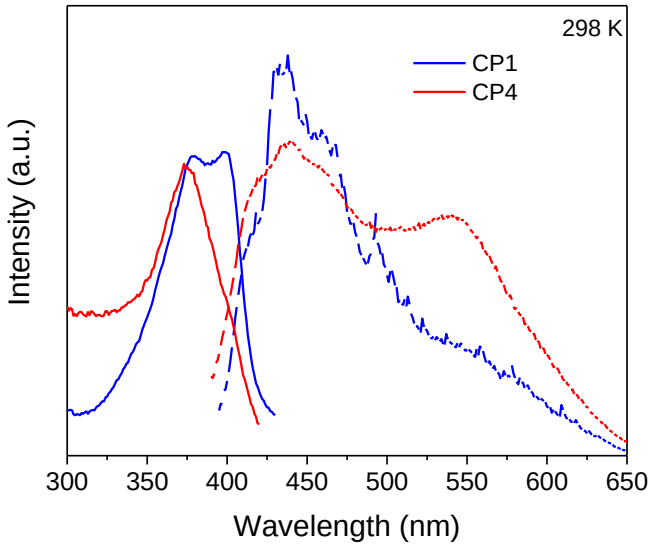

Fig. 9 Solid-state excitation (solid lines) monitored at 440 nm and emission spectra (dotted lines) of **CP1** (blue) and **CP4** (red) excited at 375 nm.

Table 1 Crystal Data, Data Collection and Structure Refinement for **CP1**, **CP2** and **CP3**.

Compound	**L1+CuI CP1**	**L1+CuI CP1**	**L1+CuBr CP2**	**L1+CuCl CP3**
Formula	$C_3H_6CuIS_2$	$C_3H_6CuIS_2$	$C_9H_{18}Br_3Cu_3S_6$	$C_3H_6ClCuS_2$
Formula weight	296.64	296.64	748.94	205.19
Temperature/K	294	100	294	294
Wavelength/Å	0.71073	0.71073	0.71073	0.71073
Crystal system	monoclinic	monoclinic	monoclinic	monoclinic
Space group	P2(1)/n	P2(1)/n	P2(1)/c	Cc
a/Å	7.6585(17)	7.5191(6)	9.5777(5)	6.9071(4)
b/Å	12.102(2)	12.1042(10)	15.3938(8)	12.5567(8)
c/Å	7.7296(16)	7.7160(7)	13.8256(8)	7.3548(4)
β/°	102.598(8)	102.861(3)	94.741(2)	97.509(2)
Volume/ Å^3	699.1(3)	684.64(10)	2031.43(19)	632.41(6)
Z	4	4	4	4
Density (calc.) g/cm^3	2.818	2.878	2.449	2.155
Absorp. coefficient/mm^{-1}	8.017	8.187	9.618	4.402
F(000)	552	552	1440	408
Crystal size/mm	0.395 × 0.115 × 0.063	0.380 × 0.142 × 0.085	0.824 × 0.136 × 0.078	1.407 × 0.346 × 0.122
Theta range for data collection/°	3.18 to 34.99	3.19 to 33.52	2.511 to 29.998	4.28 to 35.79
Index ranges	$-12 \le h \le 12$, $-19 \le k \le 19$, $-12 \le l \le 12$	$-10 \le h \le 10$, $-17 \le k \le 15$, $-10 \le l \le 10$	$-13 \le h \le 13$, $-21 \le k \le 21$, $-19 \le l \le 19$	$-10 \le h \le 10$, $-19 \le k \le 19$, $-11 \le l \le 11$
Reflections collected	33083	11411	43567	15457
Independent reflections	3076 [*R*(int) = 0.0379]	1992 [*R*(int) = 0.0315]	5943 [*R*(int) = 0.0452]	2571 [*R*(int) = 0.0436]
Refinement method	Full-matrix least-squares on F^2	Full-matrix least-squares on F^2	Full-matrix least-squares on F^2	Full-matrix least-squares on F^2
Data / restraints / parameters	3076/0/65	1992/0/65	5943/0/191	2751/2/65
Goodness-of-fit F^2	1.099	1.134	1.018	1.017
Final *R* indices [$I>2\sigma(I)$]	*R*1 = 0.0223, w*R*2 = 0.0429	*R*1 = 0.0146, w*R*2 = 0.0304	*R*1 = 0.0239, w*R*2 = 0.0412	*R*1 = 0.0227, w*R*2 = 0.543
R indices (all data)	*R*1 = 0.0285 w*R*2 = 0.0447	*R*1 = 0.0168 w*R*2 = 0.0310	*R*1 = 0.0368 w*R*2 = 0.0440	*R*1 = 0.0235 w*R*2 = 0.0548
Largest diff. peak and hole/e. Å^{-3}	0.99 and -0.77	0.56 and -0.45	0.46 and -0.60	0.37 and -0.32

Table 2 Crystal Data, Data Collection and Structure Refinement for **L2**, **CL1** and **CP4**.

Compound	**L2**	**L2+CuBr CL1**	**L2+CuI CP4**
Formula	$C_{13}H_{14}FeS_2$	$C_{15}H_{17}Br_2Cu_2FeNS_2$	$C_{26}H_{28}Cu_4Fe_2I_4S_4$
Formula weight	290.21	618.16	1342.18
Temperature/K	173	100	100
Wavelength/Å	0.71073	0.71073	0.71073
Crystal system	monoclinic	monoclinic	monoclinic
Space group	P2(1)/c	P2(1)/c	P2(1)/c
a/Å	14.6690(8)	9.8397(3)	7.2512(9)
b/Å	8.8810(6)	7.7781(3)	10.5058(13)
c/Å	9.2526(6)	24.3033(9)	22.256(3)
β /°	91.586(5)	99.9960(10)	96.086(6)
Volume/ Å^3	1204.92(13)	1831.80(11)	1685.9(4)
Z	4	4	2
Density (calc.) g/cm^3	1.564	2.241	2.644
Absorp. coefficient/mm^{-1}	1.564	7.668	7.244
F(000)	600	1200	1256
Crystal size/mm	0.300 × 0.150 × 0.100	0.248 × 0.207 × 0.048	0.489 × 0.130 × 0.082
Theta range for data collection/°	2.68 to 27.9	2.464 to 26.995	2.67 to 29.23
Index ranges	$-19 \le h \le 19$, $-11 \le k \le 11$, $-11 \le l \le 12$	$-12 \le h \le 12$, $-9 \le k \le 9$, $-30 \le l \le 31$	$-9 \le h \le 9$, $-13 \le k \le 13$, $-29 \le l \le 29$
Reflections collected	1038	25178	29368
Independent reflections	22891 [*R*(int) = 0.0395]	3985 [*R*(int) = 0.0572]	4060 [R(int) = 0.0323]
Refinement method	Full-matrix least-squares on F^2	Full-matrix least-squares on F^2	Full-matrix least-squares on F^2
Data / restraints / parameters	2891/0/145	3985/0/210	4060/0/181
Goodness-of-fit F^2	1.062	1.026	1.195
Final *R* indices [$I>2\sigma(I)$]	*R*1 = 0.0318, w*R*2 = 0.0640	*R*1 = 0.0248, w*R*2 = 0.0478	*R*1 = 0.0252, w*R*2 = 0.0596
R indices (all data)	*R*1 = 0.0414 w*R*2 = 0.0685	*R*1 = 0.0344 w*R*2 = 0.0502	*R*1 = 0.0267 w*R*2 = 0.0602
Largest diff. peak and hole/e. Å^{-3}	0.43 and -0.35	0.47 and -0.52	1.25 and -0.80

3 Conclusion

We have prepared a complete series of CuX•dithiolane CPs, which represents the first examples of crystallographically 1,3-dithiolane-ligated compounds, exhibiting a rich and uncommon structural diversity. The dimensionality and structural characteristics of these 1:1 adducts depend in a crucial manner on the nature of the μ_2-X ligand, varying from 2D to 1D. In the case of the 1D polymers, the inorganic $[Cu(\mu_2\text{-}X)Cu]_n$ ribbons are linear in the case of CuCl, but zigzagging in the case of CuBr. Another unusual material is the luminescent organometallic 1D chain of $[\{Cu_2(\mu_4\text{-}I)(\mu_2\text{-}I)\}(\mu\text{-}\mathbf{L2})]_n$ **CP4** containing both μ_4-I and μ_2-I atoms, resulting from the self-assembly reaction of CuI with the ferrocenyl-dithiolane **L2**. The impact of the nature of the halide on the structural features is again demonstrated by the structural characterization of the discrete molecular cluster $[\{Cu_4(\mu_2\text{-}Br)_2(\mu_3\text{-}Br)_2\}(\mu_2\text{-}\mathbf{L2})_2(MeCN)_2]$ (**CL1**), using CuBr under identical reaction conditions.
We are currently exploring the coordination chemistry of **L1** towards other transition metals as well as that of **L2** and its derivative Fc-C(Me)$S_2C_2H_4$, methylated at the 2-position of the dithiolane cycle.

Acknowledgements

We are grateful to the *CNRS* and the *Ministère de la Recherche et Technologie* for financial support and the region of Franche-Comté for funding a Post-doc fellowship for A. Raghuvanshi (grant RECH-MOB15-000017). We warmly thank Ms. V. Moutarlier for her help with the powder X-ray measurements. We are also expressing our gratitude to KRG, Kurdistan Regional Government, and the *Ministry of Higher Education and Scientific Research* for their financial support to N. J. Dargallay. C. Strohmann and L. Knauer thank the Deutsche Forschungsgemeinschaft *DFG* for financial support and the Fonds der Chemischen Industrie (*FCI*) for a scholarship awarded to L. Knauer.

EXPERIMENTAL SECTION

4.1 Materials and Apparatus

The CuX salts, 1,3-dithiolane, 1,2-ethanedithiol and Ferrocenecarbaldehyde were commercial obtained from Acros, Alfa Aesar and Aldrich. The ^{1}H and ^{13}C NMR spectra of **L2** were obtained on a Bruker ASCEND 400 instrument. ^{1}H chemical shifts were referenced to the proton impurity of the NMR solvent and ^{13}C chemical shifts to the NMR solvent. The poor solubility of all coordination polymers and cluster [{$Cu_4(\mu_2$-$Br)_2(\mu_3$-$Br)_2$}(μ-**L2**)$_2$($MeCN)_2$] hampered the recording of NMR spectra and luminescence spectra in solution. The solid-state emission and excitation spectra were recorded at room temperature with a Jobin-Yvon Fluorolog-3 spectrometer using a cylindrical 5 mm diameter quartz capillary with a scan speed of 1 nm/s. Infrared spectra were recorded with a 2 cm^{-1} resolution on a Bruker vertex70 FTIR spectrometer using of a Platinum ATR accessory equipped with a diamond crystal.

4.2 Preparation of CP1, CP2 and CP3

To a solution of CuI (192 mg, 1.0 mmol) in acetonitrile (10 mL) was added **L1** (299 mg, 1.1 mmol). Partial precipitation of the white product occurred after several minutes. The mixture was first stirred 1h at room temperature. The mixture was then refluxed for 5 min until the material redissolved partially. The solution was then allowed to reach slowly room temperature. After several hours, colorless crystals appeared and were filtered off after one day. Yield: 81%. IR (ATR): 2969, 2919, 1409, 1277, 1245, 1186, 1148, 1106, 1089, 983, 953, 850, 726, 691, 670, 468 cm^{-1}. Anal. Calc. for $C_{36}H_{36}Cu_2I_2S_4$ (977.85): C, 44.22; H, 3.71; S, 13.12. Found: C, 49.92; H, 3.49; S, 12.90%.

CP2 was prepared in a similar by reaction of equimolar amounts of CuBr and **L1** in MeCN solution. Yield (78%). IR (ATR): 3003, 2980, 2918, 1438, 1414, 1392, 1278, 1250, 1192, 1153, 1121, 1073, 977, 959, 856, 835, 726, 673, 660, 467 cm^{-1} Anal. Calc. for $C_{36}H_{36}Br_2Cu_2S_4$ (883.85): C, 48.92; H, 4.10; S, 14.51. Found: C, 48.52; H, 3.89; S, 14.40%.

CP3 was prepared in a similar by reaction of equimolar amounts of CuCl and **L1** in MeCN solution. Yield (78%). IR (ATR): 2987, 2969, 2923, 1413, 1397, 1272, 1242, 1189, 1143, 1115, 1075, 981, 956, 859, 838, 722, 664, 469 cm^{-1}. Anal. Calc. for $C_{36}H_{36}Br_2Cu_2S_4$ (883.85): C, 48.92; H, 4.10; S, 14.51. Found: C, 48.52; H, 3.89; S, 14.40%.

4.3 Synthesis of L2

A toluene solution of ferrocenecarboxaldehyde (214 mg, 1 mmol) and 1,2-ethanedithiol (113 mg, 1.2 mmol) was stirred at 60 ^oC with *p*-toluenesulfonic acid monohydrate (19 mg, 0.1 mmol) as a catalyst. After 24h, the solvent was evaporated and the reaction mixture subjected to column chromatography and the product was purified using hexane/dichloromethane as eluent. Yield: 203 mg, 70%, mp. 100-102 °C. ^1H NMR ($CDCl_3$) δ (ppm): 3.25-3.29 (m, 2H, $C\underline{H}_2S$), 3.34-3.43 (m, 2H, $C\underline{H}_2S$), 4.18 (s, 2H, $C_5\underline{H}_4$), 4.22 (s, 5H, $C_5\underline{H}_5$), 4.33 (s, 2H, $C_5\underline{H}_4$), 5.58 (s, 1H, $SC\underline{H}S$). ^{13}C NMR ($CDCl_3$) δ (ppm): 39.8 (SCH_2), 53.1 (CHS), 67.6, 68.4, (C_5H_4), 69.0 (C_5H_5), 88.7 (*ipso*-Fc). IR (ATR): 3089, 2962, 2920, 2851, 1784, 1754, 1727, 1689, 1665, 1640, 1414, 1390, 1264, 1227, 1180, 1127, 1102, 1035, 1022, 996, 952, 625, 855, 828, 810, 764, 737, 684, 604, 499, 482, 425, 410 cm^{-1}.

4.4 Preparation of CP4

To a solution of **L2** (29 mg, 0.1 mmol) in acetonitrile (10 mL) was added an acetonitrile solution of CuI (38 mg, 0.2 mmol). After stirring for 2h, an orange precipitate was obtained, which was redissolved by heating. The solution was cooled to room temperature and then kept at 5°C. Overnight standing gave orange crystals, which were filtered off and air-dried to give **CP4** (48 mg, 71 % yield). Anal. Calc. for $C_{26}H_{28}Cu_4Fe_2I_4S_4$ (1342.26): C, 23.26; H, 2.10; S, 9.56. Found: C, 23.62; H, 2.38; S, 9.29%. IR (ATR): 3100, 3079, 2956, 2926, 1639, 1437, 1421, 1406, 1388, 1369, 1286, 1270, 1256, 1233, 1166, 1138, 1129, 1103,1039, 1024, 998, 977, 952, 923, 913, 882, 857, 845, 829, 811, 764, 724, 702, 692, 667, 612, 493, 481, 471 cm^{-1}.

4.5 Preparation of CL1

To a solution of **L2** (145 mg, 0.5 mmol) in acetonitrile (7 mL) was added solid CuBr (143 mg, 1.0 mmol). After stirring for 10 min, the onset of the precipitation of an orange

product was noticed. The precipitate was redissolved by heating for 5 min. After allowing to reach room temperature, the solution was kept overnight at 5°C giving orange crystals of **CL1**, which were filtered off (85 mg, 68 % yield). Anal. Calc. for $C_{30}H_{34}Br_4Cu_4N_2Fe_2S_4$ (1236.36): C, 29.14; H, 2.77; N, 2.27; S, 10.37. Found: C, 28.82; H, 2.59; N, 2.07; S, 10.49%. IR (ATR): 3100, 3079, 2926, 1661, 1407, 1279, 1230, 1134, 1105, 1034, 997, 952, 924, 893, 825, 802, 776, 756, 713, 672, 608, 497, 482, 423, 412 cm^{-1}

4.6 X-ray Crystallography

X ray powder patterns were obtained at 295 K on a D8 Advance Bruker diffractometer using Ni-filtered K-α radiation. The crystal structure determinations of **CP1**-**CP4** and **CL1** were accomplished on Bruker APEX-II CCD diffractometer. Using Olex2 [52], the structures were solved with the ShelXT [53] structure solution program using Intrinsic Phasing and refined with the ShelXL [54] refinement package using Least Squares minimisation. The crystal structure determination of **L2** was accomplished on an Oxford Xcalibur Sapphire3 diffractometer; data collection: CrysAlis CCD (Oxford Diffraction, 2006); cell refinement: CrysAlis RED (Oxford Diffraction, 2006); data reduction: CrysAlis RED; absorption correction: multi-scan (CrysAlis RED; Oxford Diffraction, 2006).

The crystal data, data collection and structure refinement of all compounds are presented in Tables 1 and 2. Crystallographic data (excluding structure factors) have been deposited with the Cambridge Crystallographic Data Centre: deposition numbers CCDD 1533538 (**L2**), CCDC 1533539 (**CP2**), CCDC 1533540 (**CP3**), CCDC 1533541 (**CP1** at 294 K), CCDC 1533542 (**CP1** at 100 K), CCDC 1533543 (**CP4**), and CCDC 1533544 (**CL1**) contain detailed crystallographic data for this publication. These data may be obtained free of charge from the Cambridge Crystallographic Data Center through www.ccdc.cam.ac.uk/data_request/cif.

References

1. M. Herberhold, M. Biersack, T.E. Bitterwolf, A.L. Rheingold, Z. Naturforsch. **48b**, 161-170 (1993)

2. D.L. Hughes, J.D. Lane, R.L. Richards, C. Shortman, J. Chem. Soc., Dalton Trans. 621-626 (1994)
3. D. Schildbach, M. Arroyo, K. Lehmen, S. Martin-Barrios, L. Sierra, F. Villafane, C. Strohmann, Organometallics **23**, 3228-3238 (2004)
4. B.K. Maiti, H. Goerls, O. Klobes, W. Imhof, Dalton Trans. **39**, 5713-5720 (2010)
5. R. Uson, A. Laguna, M. Laguna, B.R. Manzano, P.G. Jones, G.M. Sheldrick, J. Chem. Soc., Dalton Trans. 285-292 (1984)
6. B. Noren, A. Oskarsson, Acta Chem. Scand. **A39**, 701-709 (1985)
7. H. Mälger, F. Olbrich, J. Kopf, D. Abeln, E. Weiss, Z. Naturforsch. **47b**, 1276-1280. (1992)
8. S. Ahrland, K. Dreisch, B. Noren, A. Oskarsson, Mater. Chem. Phys. **35**, 281-289 (1993)
9. M.D. Dembo, L.E. Dunaway, J.S. Jones, E.A. Lepekhina, S.M. McCullough, J.L. Ming, X. Li, F. Baril-Robert, H.H. Patterson, C.A. Bayse, R.D. Pike, Inorg. Chim. Acta **364**, 102-114 (2010)
10. K.M. Henline, C. Wang, R.D. Pike, J.C. Ahern, B. Sousa, H.H. Patterson, A.T. Kerr, C.L. Cahill, Cryst. Growth Des. **14**, 1449-1458 (2014)
11. P.D. Harvey, M. Knorr, J. Inorg. Organomet. Polym. Mat. **26**, 1174-1197 (2016)
12. E.W. Ainscough, A.M. Brodie, J.M. Husbands, G.J. Gainsford, E.J. Gabe, N.F. Curtis, J. Chem. Soc., Dalton Trans. 151-158 (1985)
13. K. Brodersen, W. Rölz, Chem. Ber. **110**, 1042-1046 (1977)
14. H. Braunwarth, P. Lau, G. Huttner, M. Minelli, D. Guenauer, L. Zsolnai, I. Jibril, K. Evertz, J. Organomet. Chem. **411**, 383-394 (1991)
15. A. Gryff-Keller, P. Szczeciński, H. Koziel, Magn. Reson. Chem. **26**, 468-470 (1988)
16. E.W. Abel, K.G. Orrell, K.B. Qureshi, V. Sik, Polyhedron **9**, 703-711 (1990)
17. H. Zhang, S.R. Gondi, D.Y. Son, Acta Cryst. **E62**, m3086-m3088 (2006)
18. H.N. Peindy, F. Guyon, A. Khatyr, M. Knorr, C. Strohmann, Eur. J. Inorg. Chem. 1823-1828 (2007)
19. M. Knorr, F. Guyon, A. Khatyr, C. Daeschlein, C. Strohmann, S.M. Aly, A.S. Abd-El-Aziz, D. Fortin, P.D. Harvey, Dalton Trans. 948-955 (2009)
20. M. Knorr, F. Guyon, A. Khatyr, M. Allain, S.M. Aly, A. Lapprand, D. Fortin, P.D. Harvey, J. Inorg. Organomet. Polym. Mat. **20**, 534-543 (2010)
21. M. Knorr, F. Guyon, M.M. Kubicki, Y. Rousselin, S.M. Aly, P.D. Harvey, New J. Chem. **35**, 1184-1188 (2011)

22. M. Knorr, F. Guyon, A. Khatyr, C. Strohmann, M. Allain, S.M. Aly, A. Lapprand, D. Fortin, P.D. Harvey, Inorg. Chem., **51**, 9917-9934 (2012)
23. A. Bonnot, F. Juvenal, A. Lapprand, D. Fortin, M. Knorr, P.D. Harvey, Dalton Trans. **45**, 11413-11421 (2016)
24. M. Knorr, A. Khatyr, A. Dini Aleo, A. El Yaagoubi, C. Strohmann, M.M. Kubicki, Y. Rousselin, S.M. Aly, D. Fortin, A. Lapprand, P.D. Harvey, Cryst. Growth Des. **14**, 5373-5387 (2014)
25. M. Chaabéne, A. Khatyr, M. Knorr, M. Askri, Y. Rousselin, M.M. Kubicki, Inorg. Chim. Acta **451**, 177-186 (2016)
26. M. Knorr, F. Guyon, Luminescent oligomeric and polymeric copper coordination compounds assembled by thioether ligands, in *Macromolecules containing metal and metal-like elements, vol 10: photophysics and photochemistry of metal-containing polymers*, ed. by A.S.A.-E. Aziz, C.E. Carraher, P.D. Harvey, C.U. Pittmann, M. Zeldin (Wiley, Hoboken, NJ, New York, 2010) pp. 89–158
27. U. Siemeling, U. Vorfeld, B. Neumann, H.-G. Stammler, Chem. Commun. 1723-1724 (1997)
28. W.-W. Fu, X. Gan, C.-M. Che, Q.-Y. Cao, Z.-Y. Zhou, N.N.-Y. Zhu, Chem. Eur. J. **10**, 2228-2236 (2004)
29. N. Kuganathan, J.C. Green, Chem. Commun. 2432-2434 (2008)
30. Y.-C. Yang, S.-T. Lin, W.-S. Chen, J. Chem. Research, 280-284 (2008).
31. J.C. Barnes, J.D. Paton, A. McKissock, Acta Cryst. **C39**, 547-550 (1983)
32. M.R. Baumgartner, H. Schmalle, E. Dubler, Inorg. Chim. Acta **252**, 319-331 (1996)
33. W. Ji, J. Qu, S. Jing, D. Zhu, W. Huang, Dalton Trans. **45**, 1016-1024 (2016)
34. R. Pietschnig, Chem. Soc. Rev. **45**, 5216-5231 (2016)
35. S. Clement, L. Guyard, M. Knorr, F. Villafane, C. Strohmann, M.M. Kubicki, Eur. J. Inorg. Chem. 5052-5061 (2007)
36. N. Mézailles, P.L. Floch, K. Waschbüsch, L. Ricard, F. Mathey, C.P. Kubiak, J. Organomet. Chem., **541**, 277-283 (1997)
37. H.-W. Kuai, X.-C. Cheng, D.-H. Li, T. Hu, X.-H. Zhu, J. Solid State Chem., **228** (2015) 65-75 (2015)
38. E.W. Emerson, M.F. Cain, M.D. Sanderson, C.B. Knarr, D.S. Glueck, J.C. Ahern, H.E. Patterson, A.L. Rheingold, Inorg. Chim. Acta, **427**, 168-172 (2015).
39. M.R. Churchill, K.L. Kalra, Inorg. Chem. **13**, 1427-1434 (1974)

40. J.C. Dyason, L.M. Engelhardt, C. Pakawatchai, P.C. Healy, A.H. White, Aust. J. Chem. **38**, 1243-1250 (1985)
41. L.M. Engelhardt, P.C. Healy, J.D. KIildea, A.H. White, Aust. J. Chem. **42**, 107-113 (1989)
42. J. Xiang, Y.-G. Yin, P. Mei, Inorg. Chem. Commun. **10**, 1168-1171 (2007)
43. L. Li, H.-Y. Li, Z.-G. Ren, J.-P. Lang, Eur. J. Inorg. Chem. 824-830 (2014)
44. M. Knorr, A. Bonnot, A. Lapprand A. Khatyr, C. Strohmann, M. M. Kubicki, Y. Rousselin, P.D. Harvey, Inorg. Chem., **54**, 4076-4093 (2015)
45. P. Harvey, M. Knorr, J. Clust. Sci. **26**, 411-459 (2015)
46. P.C. Ford, E. Cariati, J. Bourassa, Chem. Rev. **99**, 3625-3648 (1999)
47. T.H. Kim, Y.W. Shin, S.S. Lee, J. Kim, Inorg. Chem. Commun., **10**, 11-14 (2007)
48. P.D. Harvey, M. Knorr, Macromol. Rapid Commun. **31**, 808-826 (2010)
49. E. Cariati, E. Lucenti, C. Botta, U. Giovanella, D. Marinotto, S. Righetto, Coord. Chem. Rev. **306**, 566–614 (2016)
50. K. Tsuge, Y. Chishina, H. Hashiguchi, Y. Sasaki, M. Kato, S. Ishizaka, N. Kitamura, Coord. Chem. Rev. **306**, 636–651(2016)
51. S. Perruchas, C. Tard, X.F. Le Goff, A. Fargues, A. Garcia, S. Kahlal, J.-Y. Saillard, T. Gacoin, J.-P. Boilot, Inorg. Chem., **50**, 10682-10692 (2011)
52. O.V. Dolomanov, L.J. Bourhis, R.J, Gildea, J.A.K, Howard, H. Puschmann, J. Appl. Cryst. **42**, 339-341 (2009).
53. G.M. Sheldrick, Acta Cryst. **A71**, 112–122 (2015)
54. G.M. Sheldrick, Acta Cryst. **C71**, 3–8 (2015)